Neurobiology of Disease 108 (2017) 140–147

Contents lists available at ScienceDirect

Neurobiology of Disease

journal homepage: www.elsevier.com/locate/ynbdi

Continues administration of Nano-PSO significantly increased survival of genetic CJD mice

Orli Binyamin [a,b], Guy Keller [a,b], Kati Frid [a,b], Liraz Larush [c], Shlomo Magdassi [c], Ruth Gabizon [a,*]

[a] Department of Neurology, The Agnes Ginges Center for Human Neurogenetics, Hadassah University Hospital, 91120 Jerusalem, Israel
[b] Medical School, The Hebrew University, Jerusalem, Israel
[c] Casali Institute of Chemistry, The Hebrew University of Jerusalem, Jerusalem 91904, Israel

ARTICLE INFO

Article history:
Received 8 May 2017
Revised 20 August 2017
Accepted 21 August 2017
Available online 25 August 2017

Keywords:
Prions
GAGs
Nanotechnology
Genetic
Pomegranate
Nano-PSO

ABSTRACT

We have shown previously that Nano-PSO, a nanodroplet formulation of pomegranate seed oil, delayed progression of neurodegeneration signs when administered for a designated period of time to TgMHu2ME199K mice, modeling for genetic prion disease. In the present work, we treated these mice with a self-emulsion formulation of Nano-PSO or a parallel Soybean oil formulation from their day of birth until a terminal disease stage. We found that long term Nano-PSO administration resulted in increased survival of TgMHu2ME199K lines by several months. Interestingly, initiation of treatment at day 1 had no clinical advantage over initiation at day 70, however cessation of treatment at 9 months of age resulted in the rapid loss of the beneficial clinical effect. Pathological studies revealed that treatment with Nano-PSO resulted in the reduction of GAG accumulation and lipid oxidation, indicating a strong neuroprotective effect. Contrarily, the clinical effect of Nano-PSO did not correlate with reduction in the levels of disease related PrP, the main prion marker. We conclude that long term administration of Nano-PSO is safe and may be effective in the prevention/delay of onset of neurodegenerative conditions such as genetic CJD.

1. Introduction

We have shown previously that administration of Nano-PSO, a nanodroplet formulation of pomegranate seed oil (PSO), significantly delayed disease progression in transgenic mice modeling for genetic prion disease linked to the E200K PrP mutation (Mizrahi et al., 2014). TgMHu2ME199K mice express human-mouse chimeric E199K PrP on a null (for homozygous) or a wt PrP (for heterozygous) C57BL/6 background (Friedman-Levi et al., 2011). Mice from both lines suffer from their first neurological symptoms at as early as 5–6 month of age and deteriorate progressively to a terminal condition at about 12–15 months of age (Friedman-Levi et al., 2013; Friedman-Levi et al., 2011). TgMHu2ME199K mice also exhibit classical features of neurodegeneration (Kovacs et al., 2010; Fainstein et al., 2016), such as progressive reduction in cortical neurons and synapses starting at 4–6 months, decreased neurogenesis and impaired hippocampal-dependent memory. It is therefore possible that the beneficial effect of Nano-PSO relates to features common to several neurodegenerative diseases.

PSO comprises a unique component, Punicic acid (PA), also designated as Omega 5, a conjugated polyunsaturated fatty acid considered one of the strongest natural antioxidants. Unsaturated fatty acids such as PA were shown to readily cross the blood brain barrier (BBB) (Avellini et al., 1994; Dhopeshwarkar and Mead, 1973; Spector, 1988). To increase its bioavailability and activity, we generated water soluble nano-emulsions of PSO, denominated Nano-PSO (Sawant and Torchilin, 2010). In our previous work, Nano-PSO was administered to TgMHu2ME199K from day 70 (asymptomatic mice) to day 270 (sick) (Mizrahi et al., 2014). Concomitant with the Nano-PSO dependent delay of disease advance, brains from treated mice exhibited decreased lipid oxidation and reduced neuronal loss, as well as increased neurogenesis (Mizrahi et al., 2014). Nano-PSO also reduced disease burden and oxidation of lipids in experimental autoimmune encephalomyelitis (EAE), a rodent model of Multiple Sclerosis (Binyamin et al., 2015).

In the present work, we tested whether lifelong administration of a self-emulsion formulation of Nano-PSO can increase the survival of TgMHu2ME199K/WT and TgMHu2ME199K/KO mice, mimicking for heterozygous or homozygous carriers of the E200K mutation. As a control experiment, groups of both TgMHu2ME199K mice lines were treated with a parallel Nano-Soybean oil formulation (Nano-SBO). In addition, Nano-PSO was administered to a group of wt mice for 180 days, and followed for their general status. Brains from Tg mice treated with both compounds at disease end point (score 4, see

* Corresponding author at: Department of Neurology, The Agnes Ginges Center for Human Neurogenetics, Hadassah University Hospital, Jerusalem 91120, Israel.
E-mail address: gabizonr@hadassah.org.il (R. Gabizon).
Available online on ScienceDirect (www.sciencedirect.com).

http://dx.doi.org/10.1016/j.nbd.2017.08.012
0969-9961/

Table 1
Score of disease sign in transgenic mice.

Score	Disease sign
1	Initial hind limb weakness
1.5	Partial hind limb weakness
2	Significant hind limb weakness/paralysis
2.5	+ Legs clasping
3	+ Full paralysis in one limb
3.5	+ Significant weakness at the other hind foot
4	Full paralysis in both limbs (end point)

Table 1) and designated time points were tested for the accumulation of disease related PrP and additional pathological features.

We found that life-long administration of Nano-PSO significantly increased the survival of TgMHu2ME199K mice while it was not toxic to both TgMHu2ME199K and wt mice. Pathological examinations of Nano-PSO treated brains versus the placebo formulation indicated that both disease advance and the beneficial effect of Nano-PSO correlated with the levels of sulfated sugars in neuronal cells, and not with those of disease related PrP.

2. Materials and methods

2.1. Generation of Nano-PSO and Nano-SBO self-emulsifying formulations, as described in patent no. 14/523,408

Pomegranate oil (31.46%), Tween 80 (44.05%), Span 80 (19.51%) and ethanol (4.972%) were added to a 250 ml beaker (chemical glass), and mixed by a magnetic stirrer (4.5 cm) for 4 h. Next, 10 μl of the mixture were added to 3 ml of deionized water. The O/W nano-emulsion droplets size was: 224 nm Z Average, peak 1: 181 nm, 100%; Pdi: 0.389 (average of 10 measurements).

2.2. Preparation of Nano-PSO and Nano-SBO aqueous solution

Nano-PSO or Nano-SBO (16.5 ml) self-emulsion formulations were diluted in 300 ml of water to form a white emulsion with a final concentration of 1.6% oil. Mice were allowed to drink freely. The amount of water consumed by the mice was equivalent for all experimental (PSO) versus control (SBO) groups for the duration of the study. For most of the experiments, mice drank between 3 and 4 ml a day, as measured by the total reduction of volume for each cage. However, very sick mice (score 3 or more) drank 10% less water regardless of the treatment.

2.3. Animal experiments

All animal experiments were conducted under the guidelines and supervision of the Hebrew University Ethical Committee, which approved the methods employed in this project (Permit Number: MD-15-14462-5).

2.3.1. Treatment of TgMHu2ME199K mice

Nano-PSO and Nano-SBO were administrated to new born mice (until 3 weeks of age) by dripping gently into their mouth 5 times a week. For older mice, Nano-PSO and Nano-SBO were added to their drinking water. Mice were sacrificed at designated time points when required by the experimental protocol or at score 4. Brains and eyes were processed for pathological and biochemical experiments.

2.4. Mice scoring system for disease signs

TgMHu2ME199K mice were followed twice a week for the appearance of spontaneous neurological disease. Mice were scored for disease severity and progression according to the next scale: no clinical score = 0; initial hind limb weakness presented by smaller legs spread, lower body position and gentle assembly of hind limbs while walking = 1; partial hind limb weakness = 1.5; significant hind limb/s weakness or paralysis = 2; significant hind limb/s weakness or paralysis with significant legs clasping = 2.5; full paralysis in one limb = 3; full paralysis in one limb and weakness at the other hind foot = 3.5; full paralysis in both limbs = 4. Any other sign of illness such as hunchback or glued fur added 0.5 point to the score. Mice were sacrificed at designated time points or when they were too sick or paralyzed to reach food and water, or after losing 20% body weight, according to the ethical requirements of the Hebrew University Animal Authorities.

2.5. Statistical studies

Analyses of score graphs were performed with the Microsoft Excel software (2010). Graphs represent the mean and respective standard error of clinical scores of groups of mice. The differences between experimental groups were assessed by one-way analysis of variance followed by the paired two-tailed Student's *t*-test. Kaplan-Meier analyses were performed to evaluate the survival until score 2.5 and 4, the differences between the groups were assessed by the log-rank test (Mantal-Cox) to estimate the chi-squared test.

2.6. Pathological examinations and immunocytochemistry)

Histological evaluations were performed on paraffin-embedded sections of brain and occasionally retina samples. Sections were stained with Alcian blue/Periodic Acid Schiff (EMD Millipore, Billerica, MA, USA) to assess sugar polymer detection; with α-PrP pAb RTC antibody to evaluate the levels of PrP accumulation (Canello et al., 2010; Mizrahi et al., 2014) and with mAb EO6 (Avanti) to evaluate the levels of lipid oxidation (Palinski et al., 1996).

2.7. Western blot analysis

Brain extracts from TgMHu2ME199K mice at the designated time points were homogenized at 10% (W/V) in 10 mM Tris–HCl, pH 7.4 and 0.3 M sucrose. For Proteinase K digestions, 200 μg of 10% brain homogenates were extracted with 2% sarcosyl on ice before incubation with 20 mg/ml Proteinase K for 30 min at 37 °C. Samples were subsequently boiled in the presence of SDS, subjected to SDS PAGE and immunoblotted with α-PrP pAb RTC (Canello et al., 2010).

3. Results

3.1. Administration of a self-emulsion formulation of Nano-PSO to TgMHu2ME199K mice

In our previous publications, we treated TgMHu2ME199K mice with a Nano-PSO formulation prepared by sonication (Mizrahi et al., 2014), and compared the clinical results to those of untreated Tg mice. For the present work, and as part of a project to produce a water free formulation of Nano-PSO that can be encapsulated in soft gel capsules, we generated a self-emulsion formulation of PSO and appropriate emulsifiers (see methods). This mixture, upon dilution into water or a stomach similar solution, forms droplets of 200–300 nm, as is the case for the sonicated Nano-PSO. A similar formulation comprising soybean oil (SBO) was prepared and used as a placebo for these experiments. Nano-PSO and Nano-SBO formulations were diluted into the mice drinking water. Newborn TgMHu2ME199K mice either on a PrP ablated or a wt PrP background were initially feed by dripping the solution gently into their mouth. From 3 weeks of age onward, mice were allowed to drink freely. The amount of water consumed was equivalent for all PSO and SBO groups of mice for the duration of the study. For most of the experiments, mice drank between 3 and 4 ml a day, as measured by the

total reduction of volume for each cage. However, very sick mice (score 3 or more) drink 10% less water regardless of the treatment.

Mice were scored twice weekly for clinical signs of disease as described in the methods and sacrificed either when they were diagnosed with score 4, or otherwise when they reached 18 months of age with a lower score (which was the case for 50% of the Nano-PSO treated mice) (see Table 1 for description of clinical signs as related to scores). Fig. 1a depicts the advance of the clinical score over time for all groups. As can be seen in the figure, there was no significant difference in disease advance between Nano-SBO treated TgMHu2ME199K/KO and TgMHu2ME199K/WT mice. Moreover, the rate of disease advance in these groups was also similar to that of the untreated mice in previous experiments (see inserted graph in Fig. 1a) (Mizrahi et al., 2014). Also, the decrease in the rate of disease aggravation following Nano-PSO treatment was only slightly different for TgMHu2ME199K mice on wt as compared to PrP ablated background for the total of the mice life span. Indeed, from day 150 and onward, the rate of disease aggravation increased significantly for the placebo groups as compared to the Nano-PSO treated groups, the difference becoming statistically significance from the first period of the disease appearance and until the end of the experiments (Table 2). A control group of C57BL/6 wt mice (yellow line) were also treated with Nano-PSO for 18 months and did not show any adverse effects.

Fig. 1b and c depict a Kaplan-Mayer analysis of the clinical results for 2 individual score points (see Table 1). Since there was no statistical difference for disease advance between both Tg lines for both the Nano-PSO and the placebo treated groups, we pulled the results together for sections b and c. Fig. 1b presents the results for score 2.5, when the sick TgMHu2ME199K mice first clasp their legs, while Fig. 1c does the same for score 4, when mice are mostly paralyzed and have to be sacrificed according to the ethical permit for these experiments. As can be seen in the graphs, there was a large difference between the median for the Nano-PSO and the placebo treated groups for both score points (136 days for score 2.5 and >140 days for score 4; $p < 0.0001$, $\chi^2 = 17.72$). Indeed, Fig. 1c shows that when all mice in the placebo groups were already dead, 50% of the Nano-PSO treated mice were still alive until the end point of the experiment (18 months), indicating a significant increase in survival ($p < 0.0001$, $\chi^2 = 17.05$). Our results therefore indicate that while administration of Nano-PSO for the life span of TgMHu2ME199K mice could not inhibit the outbreak of disease, it did delay aggravation and death in the absence of any side effects.

To determine whether the clinical effect of Nano-PSO requires chronic administration of the formulation or otherwise produces a constant beneficial effect after a designated period of treatment, treatment with Nano-PSO was stopped for some of the mice at 9 month of age (263 days), and scoring was resumed for this group 6 weeks later. Fig. 2 analyses the differences between the disease scores for all experimental groups at 7, 9, and 10 months of age. This includes parallel groups from our previous manuscript (Mizrahi et al., 2014), when Nano-PSO prepared by sonication was administrated to TgMHu2ME199K mice from 70 to 270 days. Several important conclusions can be drawn from these results. First, the clinical effect of Nano-PSO on the TgMHu2ME199K mice was the same when treatment commenced at birth or at 70 days with either of the formulations (sonicated

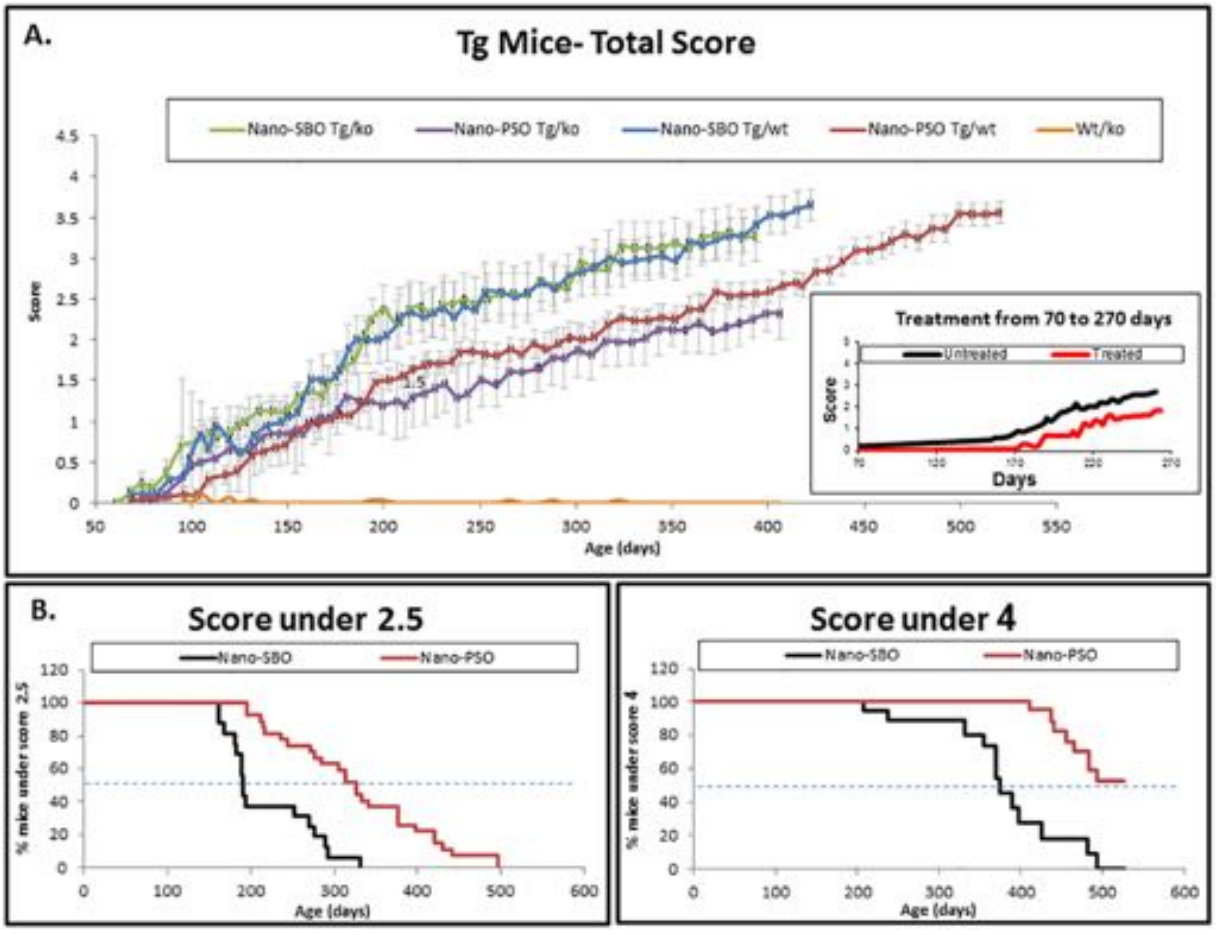

Fig. 1. Lifelong administration of Nano-PSO to TgMHu2ME199K mice significantly increased their survival. Nano-PSO (19 tg/wt mice, 11 tg/ko mice, 13 wt/ko mice) or Nano-SBO (10 tg/wt mice, 9 tg/ko) were administered to TgMHu2ME199K mice from birth. Mice were scored for disease signs as described in Table 1. A. Average group score as related to age of mice. B. Percentage of mice under score 2.5 as related to age of mice. C. survival curve: Percentage of mice under score 4 as related to age of mice. Inserted graph in panel (A) was copied from our previous work (Mizrahi et al., 2014), presenting score of Nano-PSO treatment of TgMHu2ME199K mice from 70 days to 270 days.

Table 2
Statistical analysis of results described in Fig. 1.

Experimental groups	Asymptomatic period score 1 (60–120 days)	First disease signs appearance score 1–2.5 (120–210 days)	High severity of disease signs score 2.5–4 (210–420 days)
Tg/ko (nano-PSO VS nano-soya)	*p < *0.004*	*p < *0.00001*	*p < *0.00001*
Tg/wt (nano-PSO VS nano-soya)	*p < *0.004*	*p < *0.004*	*p < *0.00001*
Tg/ko VS Tg/wt (nano-soya)	No difference	No difference	No difference
Tg/ko VS Tg/wt (nano-PSO)	*p < *0.05*	No difference	*p < *0.001*
Total nano-PSO VS nano-soya	*p < ***0.003***	*p < ***0.001***	*p < ***0.00001***

* Statistically significant.

and self-emulsion), at least for the aggravation until the 9 months' time point. This may infer that Nano-PSO interferes with the ongoing oxidation damage but cannot prevent very early molecular events that eventually lead to the fatal outcome. Consistent with such hypothesis, Fig. 2 also shows that following termination of treatment at 9 months of age, mice deteriorated to the score values of the Nano-SBO group quite fast, again indicating Nano-PSO does not "cure" the neurodegenerative process, but rather keeps the level of the damage under control, maybe by reducing the levels of ROS formed by the pathological process. This also infers that Nano-PSO treatment should be given chronically.

3.2. The beneficial effect of Nano-PSO is independent from PK resistant PrP accumulation

PK resistant PrP first appears in brains of the TgMHu2ME199K mice at very low levels at 1–3 months of age and continues to accumulate further until 7–9 month old (Friedman-Levi et al., 2013; Friedman-Levi et al., 2011). In our previous publication (Mizrahi et al., 2014), we tested the levels of PK resistant PrP in TgMHu2ME199K mice treated with Nano-PSO from 70 to 270 days by immunoblotting, and found no reduction in PrP levels as compared to untreated mice that correlated with the improved clinical status of the treated mice, at least at that time point. We now show that the dissociation of disease state from PrP levels was also true for different time points of treated and untreated mice. Fig. 3a shows the levels of total and PK resistant PrP in Nano-PSO and placebo treated mice at 9, 12, and 14 months old mice. All together these brains represent TgMHu2ME199K mice suffering from genetic prion disease at scores from 1.5 to 4; or in other words from light disease (Partial hind limb weakness) to terminal stage. Regardless of the vast difference in the clinical status of these mice, the brain levels of PK resistant PrP was very similar in all of them. This probably indicates that while the formation of PK resistant PrP from mutant PrP may be the trigger for a series of events leading to disease presentation and aggravation, the actual PrP^{Sc} levels may not correlate with disease advance, with or without Nano-PSO treatment. Consistent results can be seen in Fig. 3b, in which paraffin sections of brains from Nano-PSO and placebo treated Tg mice were immunostained with α PrP pAb RTC after an antigen retrieval procedure but without PK digestion, a procedure that detects disease related PrP forms (Kovacs et al., 2010). Interestingly, while Fig. 3b did not present any difference in the levels of disease related PrP accumulation over time and as related to treatment, it does show a significant higher accumulation of the hematoxylin - counter stain in the placebo groups at ages 7 m–13 m as compared to the Nano-PSO treated mice. A strong counter stain is a well-known marker of sick cells about to die by an apoptotic pathway (Liu et al., 2015; Sharma et al., 2016). Moreover, the dying cells in the hippocampus of the placebo treated mice from 11 months onward seem to have lost most of their axons, while this was not the case for the Nano-PSO treated mice.

3.3. Nano-PSO inhibits the accumulation of alcian blue stained amyloid sugars

Glycosaminoglycans (GAGs) are frequently found associated with proteinaceous deposits in tissues of patients affected by amyloid related neurodegenerative diseases, as is the case for CJD and AD (Diaz-Nido et al., 2002; Snow et al., 1989; Yin et al., 2007). Experimental evidence indicates that these molecules can play an active role in favoring amyloid fibril formation and stabilization, as is the case for GAGs helping to increase the levels of PK resistant PrP in diverse -Protein Misfolding Cyclic Amplification methods (Imamura et al., 2016; Vieira et al., 2014; Wong et al., 2001). In prion disease as well as in other neurodegenerative conditions (Papy-Garcia et al., 2011), the role of GAGs has been studied extensible. Among other facts, it was shown that PrP^{Sc} may be internalized into lysosomes together with GAGs and that the activity of lysosomal enzymes is impaired in prion diseases (Mayer-Sonnenfeld et al., 2008; Mayer-Sonnenfeld et al., 2005). Also, it was shown that low molecular weight sulfated sugars may compete with highly polymerized GAGs for the binding to misfolded proteins and thereby serve as anti-prion agents (Schonberger et al., 2003; Shaked et al., 2001). Most

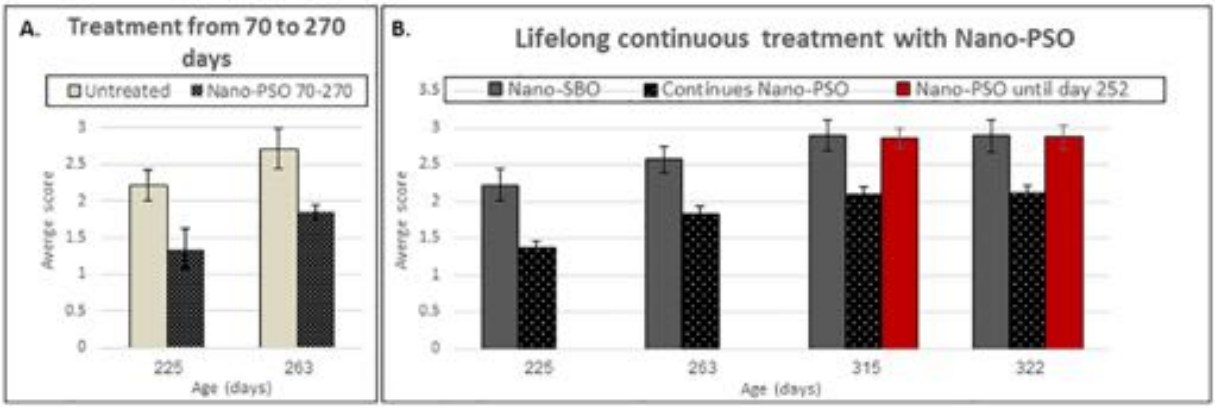

Fig. 2. Maintaining the clinical effect of Nano-PSO requires constant treatment. A. Disease score at designated time points for 70–270 days Nano-PSO treated (n = 6) and untreated (n = 6) mice B. Scores at designated time points for mice treated with Nano-PSO or Nano-SBO. In this group, treatment was discontinued for some of the Nano-PSO treated mice (n = 20), and scored for clinical signs 6 weeks later (present in the red column from day 315), presenting similar score as the Nano-SBO group. * p < 0.0005 for the discontinued sub-group versus the group treated continuously.

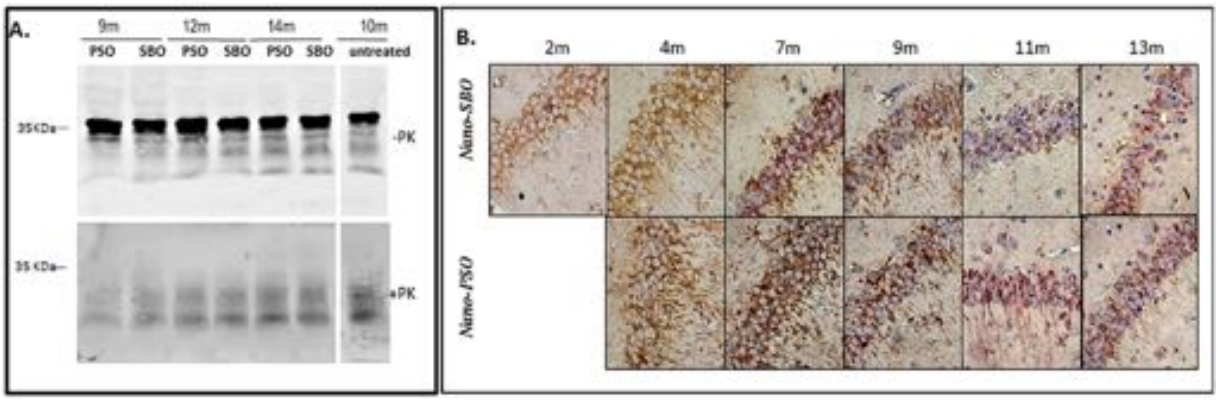

Fig. 3. Levels of disease related PrP are independent from disease progression and from Nano-PSO clinical effect. Brain samples of Nano-PSO and Nano-SBO treated TgMHu2ME199K mice at different time points were analyzed for disease related PrP accumulation. A. Western blot analysis of mice brain extracts at 9, 12 and 14 months of age. Each sample was digested in the presence or absence of PK, as described in the methods, and immunoblotted with α PrP pAb RTC. B. Time course immunohistochemical evaluation of disease related PrP accumulation in TgMHu2ME199K mice. Paraffin embedded brain slices of Nano-PSO and Nano-SBO treated Tg mice were treated for epitope revealing as described in the methods and subsequently immunostained with α PrP pAb RTC, and counter-stained with hematoxylin. Magnification of CA1 area in the hippocampus by ×40 lens.

interestingly, GAGs preferentially bind to oxidized lipids and proteins (Hijazi et al., 2005; Kaplan and Aviram, 2001). To this effect, we tested brain sections from Nano-PSO and placebo treated TgMHu2ME199K mice for alcian blue/PAS staining for GAGs (see methods). To asses if GAG accumulation in these mice brains correlate with lipid oxidation we immunostained parallel slides with mAb EO6 (Palinski et al., 1996), which recognizes oxidized phospholipids. We have shown previously that Nano-PSO treated brains from both TgMHu2ME199K mice, as well as EAE induced mice present a pronounced reduction of EO6 immunostaining (Binyamin et al., 2015; Mizrahi et al., 2014).

Fig. 4a shows consecutive slides from the brains stained in Fig. 3b for disease related PrP, now stained for GAGs with the alcian blue/Pas staining (Snow et al., 1989). In some cases, additional slides (Fig. 4b) were double stained for both PrP and GAGS to investigate the colocalization of both protein and sugar aggregates. As can be seen in Fig. 4a for the hippocampus, the alcian blue/PAS staining increased in the placebo treated groups concomitant with disease advance from 4 months onward. In the Nano-PSO treated group, GAGs staining started significantly later, at 7 months old mice, and at all stages thereafter the level of staining was less intense than in the parallel placebo treated mice, thereby correlating both with age related disease advance and with

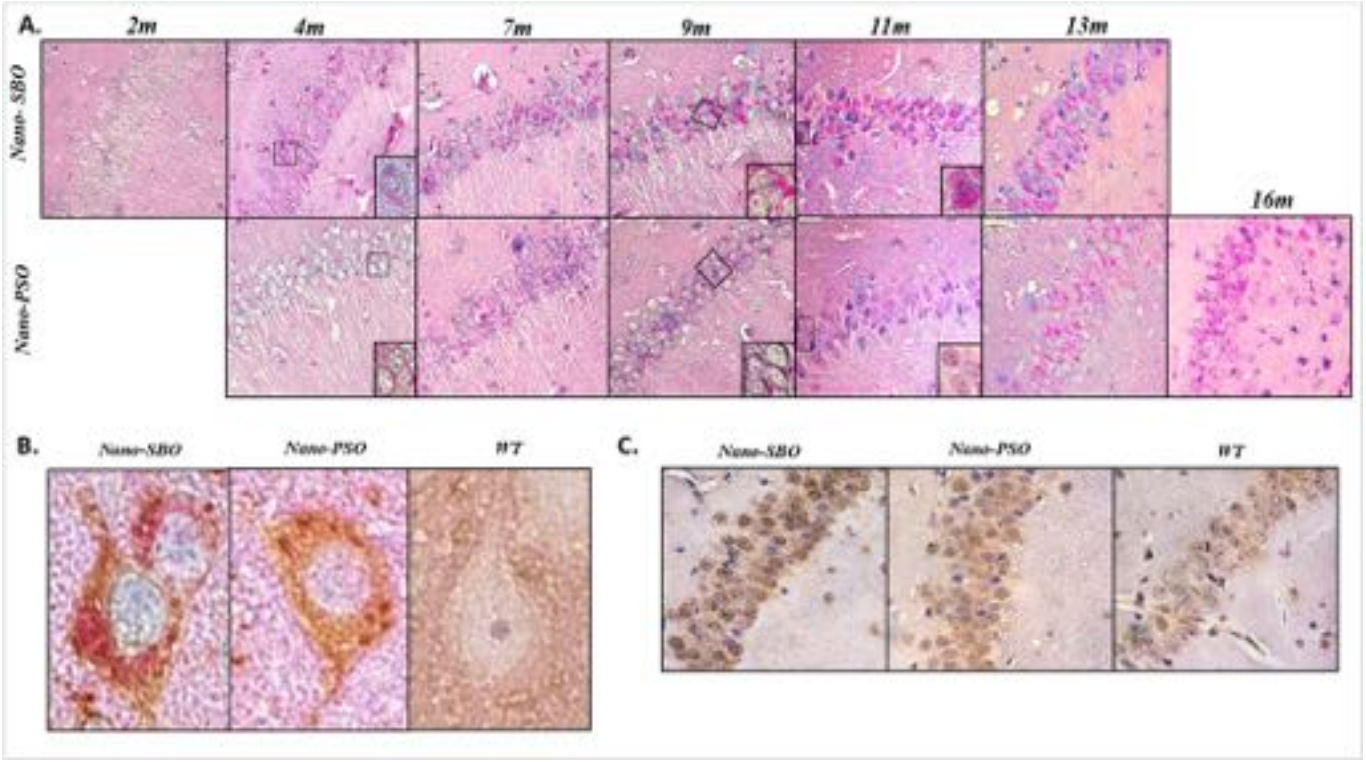

Fig. 4. Reduced levels of GAGs and lipid oxidation in the hippocampus of Nano-PSO treated TgMHu2ME199K mice. A. Paraffin embedded brain slices of TgMHu2ME199K mice at different ages from Nano-SBO (upper panel) or Nano-PSO treated group (lower panel) were stained with alcian blue/PAS for the detection of GAGs. Picture magnification is ×40, and ×60 for the enlarged inserts. B. Brain slices of 7 months old Nano-PSO and Nano-SBO treated TgMHu2ME199K mice as well as control wt/ko mice were double-stained for alcian blue/PAS (red stain) and PrP (brown stain). Magnification of single cells (×60). C. Brain slices from 9 months old mice from Nano-PSO and Nano-SBO treated TgMHu2ME199K mice were immunostained with mAb EO6 (Palinski et al., 1996), magnification ×40.

reduced disease aggravation by treatment. This is the first evidence that reduction in amyloid GAGs can be associated with a slower disease advance without a visible change in the accumulation of misfolded PrP protein in prion diseases, or the corresponding aggregated proteins in other neurodegenerative conditions. Indeed, accumulation of GAGs is known as a pathogenic factor by itself, as is the case for all genetic diseases associated with malfunction of enzymes in the diverse GAGs synthesis pathways, known as mucopolysaccharidoses (Tomatsu et al., 2013). Concomitantly with GAG reduction, Fig. 4c shows (for 9 months old brains samples stained with the EO6 antibody) that Nano-PSO treatment significantly reduced the levels of lipid oxidation in the TgMHu2ME199K mice hippocampus, suggesting that oxidized lipids may serve as a trigger for GAGs accumulation. This may explain why a brain targeted lipid antioxidant can reduce GAG levels.

Double staining for PrP and GAGs (Fig. 4b) indicates a partial colocalization of both molecules. The red staining is mostly present in cytoplasmic parts of the cells, probably in lysosomes (Suzuki et al., 1997), while disease relate PrP is seen as aggregates in these areas, but also is dispersed in other parts of the cells. As expected, no GAGs or disease related PrP can be observed in wt brains.

3.4. Reduced alcian stained retinas in Nano-PSO treated Tg mice

Retinal pathology in animals affected with prion disease was reported long ago (Ye, 2009). To this effect, we examined the accumulation of both disease related PrP (stained with α PrP pAb RTC) and sulfated sugars in the retinas of 14 months old Tg mice treated with Nano-PSO as compared to 10 months old untreated mice (of the same score that the 14 treated mice). As shown in the previous figures for the brains of such mice, also the retina of placebo treated mice, in particular the ganglion cell layer, presented extensive disease related PrP immunostaining concomitant with alcian blue/Pas staining (Fig. 5). As is the case for Nano-PSO treated brains, also the retinas from the treated mice showed significant reduction of the GAGs staining, while the immunostaining for disease related PrP remains unchanged.

4. Discussion

We have shown here that Nano-PSO administration may increase the survival of TgMHu2ME199K mice by several months. This was true for mice treated from the day of birth until they reach their fatal state and is most probably true for mice in which Nano-PSO treatment commenced at 70 days old, an age in which TgMHu2ME199K mice appear healthy but are closer to the manifestation of clinical signs. Our results also show that secession of Nano-PSO administration to TgMHu2ME199K at 9 months of age restored the rate of aggravation to that of the untreated mice very fast, indicating treatment should be continued constantly.

In addition, we demonstrated here that the levels of disease related PrP in the TgMHu2ME199K mice modeling for E200K genetic CJD were very similar from light neurological signs to fatal symptoms and that the increased survival generated by Nano-PSO administration did not result in a parallel reduction in the levels of the prion protein. Rather than that, we showed here that both age related aggravation of disease and Nano-PSO dependent increased survival, correlated with the levels of GAG accumulation as determined by alcian blue/PAS staining. GAG aggregates represent a general marker of neurodegeneration, as opposed to disease related PrP, which is a specific marker of prion diseases. We have shown previously (Mizrahi et al., 2014) that administration of Nano-PSO to TgMHu2ME199K mice may increase the levels of neurogenesis.

Several important conclusions can be drawn from these results. First, while the E200K mutation, as is the case for other pathological mutations in neurodegenerative conditions (Hinz and Geschwind, 2017), is linked to the presentation of fatal disease in older carriers of these mutations, there is no evidence that the rate of clinical progression correlates with the apparent levels of disease related PrP accumulation. Such a lack of correlation between aberrant PrP forms and clinical disease was shown in several prion systems (Czub et al., 1988; Lasmezas et al., 1997). Indeed, while it is well established that the initial conversion of PrP^{C} into PrP^{Sc} signals the initiation of the neurodegenerative process in prion diseases (Prusiner, 2013), other unknown factors may come into play thereafter (Caughey and Baron, 2006) which determine the rate of disease aggravation. In addition, it was shown years ago that the infectious activity of PrP^{Sc} may depend on its degree of aggregation and location in membranes, and not necessarily on its direct protein levels (Gabizon et al., 1987; Silveira et al., 2005). In addition, it was recently shown that aggregated PrP forms are not always related to disease and that pathology of such aggregates may depend on additional component present during the aggregation process (Wang et al., 2017). As is the case for A-beta in AD, it is actually oligomeric aggregates of PrP^{Sc} forms, even in soluble forms, that may be responsible for most of the damage (Bett et al., 2017; Lesne et al., 2013; Silveira et al., 2005). As for the E200K PrP, we have shown previously that both in this mice model and in human E200Kpatients, mutant PrP can appear in several abnormal forms, including aggregated and PK sensitive, as well as soluble and PK resistant (Friedman-Levi et al., 2013).

Consistent with the lack of association between levels of PrP accumulation and disease advance in untreated mice is the fact that the significant increased survival of TgMHu2ME199K mice resulting from Nano-PSO treatment did not correlate in any form with the levels of disease related PrP accumulation. Reduction of PrP^{Sc} in prion infected cell lines has been considered for many years as the “gold standard” for the screening of putative anti-prion agents (Kocisko and Caughey, 2006b; May et al., 2003; Peretz et al., 2001; Raymond et al., 2006; Schonberger et al., 2003). However, agents identified by this procedure where not necessarily shown to be active in clinical experiments, both in animals and in human (Geschwind et al., 2013; Kocisko and Caughey, 2006a). New reagents suggested as possible treatments are also either independent or only partially related to PrP accumulation (Halliday et al., 2017) (Zhou et al., 2015). This was also true for some agents developed for the treatment of Alzheimer's disease, in which, at least for now, reduction of A-beta brain aggregates did not result in a slower disease advance (Abbott and Dolgin, 2016).

Interestingly, we show here that Nano-PSO reduced the accumulation of GAGs as stained by alcian blue/PAS, and that it is this marker rather than PrP that correlates with disease advance. GAGs have been shown to be a component of amyloid in several neurodegenerative conditions (Diaz-Nido et al., 2002; Snow et al., 1989), including prion diseases. How Nano-PSO can interfere with the accumulation of GAGs in neurons is unknown, however, it may well be related to its antioxidant properties. GAGs were shown to bind preferentially to oxidized proteins and lipids (Kaplan and Aviram, 2001), which levels Nano-PSO can reduce significantly (see Fig. 4c) (Binyamin et al., 2015; Mizrahi et al., 2014). The antioxidative properties of Nano-PSO may also explain its neuroprotective effects, as was shown for reagents active in other neurodegenerative conditions (Velusamy et al., 2017). Accumulation of GAGs in lysosomes can cause neurodegeneration, as in the case for the mucopolysaccharidoses, a group of metabolic disorders caused by the absence or malfunctioning of lysosomal enzymes needed to break down glycosaminoglycans (Archer et al., 2014).

An interesting point revealed in this manuscript is that the maintenance of the Nano-PSO associated clinical effect requires chronic administration of the treatment. We also show here that there was no advantage in very early treatment. Together, this implies that Nano-PSO does not “cure” or inhibit the manifestation of the neurodegenerative process, but rather may control the levels of deleterious brain oxidation while it is being administrated. While this is definitely not enough to constitute a comprehensive treatment for prion and other neurodegenerative process, it may constitute an initial approach to delay disease onset in carriers of pathogenic PrP mutations as well as in subjects at risk for other neurodegenerative conditions. Additional reagents, which may well come from screening for α PrP related

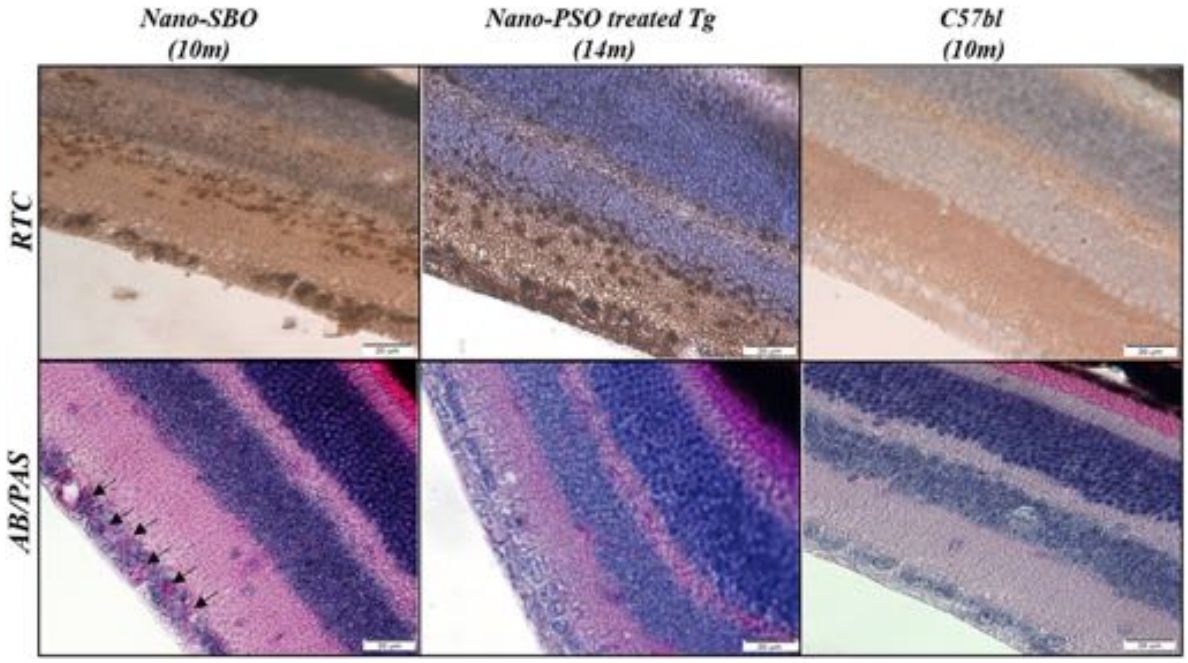

Fig. 5. Nano-PSO treatment reduced the GAG levels in retinas of treated TgMHu2ME199K mice. Paraffin embedded eyes of 10 months old C57bl and Nano-SBO treated TgMHu2ME199K mice as well as 14 months old Nano-PSO treated Tg, were immunostained for disease related PrP (A-C) and alcian blue/PAS stain (D–F). Magnification of all pictures is ×20. Arrows represent GAG accumulation in the ganglion cell layer in retina of Nano-SBO treated TgMHu2ME199K mouse.

mechanisms (Imberdis et al., 2016; Karapetyan et al., 2013; Silber et al., 2014), may constitute partners of Nano-PSO in efficient cocktails against prion diseases. Similar cocktails may latter be developed for diverse neurodegenerative conditions.

Many beneficial clinical effects have been attributed to pomegranate extracts, in particular related to the antioxidant properties of polyphenols present in the juice of the fruit (Jurenka, 2008). Some of them relate to neurological conditions, ranging from hypoxic-ischemic brain injury to Alzheimer's disease (Amri et al., 2017; Braidy et al., 2016; Loren et al., 2005; Subash et al., 2014). However, there were no previous reports about PSO and its active component, Punicic Acid, pertinent to neurological diseases before our work (Mizrahi et al., 2014). Interestingly, it has been just published that a similar nanoemulsion formulation of PSO may be effective against brain tumors (Mota Ferreira et al., 2016).

5. Conclusion

In the future, when specific, aggregated protein related drugs are generated for patients suffering from neurodegenerative diseases, Nano-PSO may serve as one of the components for a treatment or prevention cocktail. In particular since its formulation is safe and comprises only food approved ingredients.

Funding

This project was funded by a grant from the Agnes Ginges Center for Human Neurogenetics and from Granalix Biotechnologies.

Potential conflicts of interest

RG and SM are the founders of Granalix Biotechnologies, a company developing science based natural compounds, which is partially financed this study.

References

Abbott, A., Dolgin, E., 2016. Failed Alzheimer's trial does not kill leading theory of disease. Nature 540, 15–16.

Amri, Z., et al., 2017. Effect of pomegranate extracts on brain antioxidant markers and cholinesterase activity in high fat-high fructose diet induced obesity in rat model. BMC Complement. Altern. Med. 17, 339.

Archer, L.D., et al., 2014. Mucopolysaccharide diseases: a complex interplay between neuroinflammation, microglial activation and adaptive immunity. J. Inherit. Metab. Dis. 37, 1–12.

Avellini, L., et al., 1994. Linoleic acid passage through the blood-brain barrier and a possible effect of age. Neurochem. Res. 19, 129–133.

Bett, C., et al., 2017. Enhanced neuroinvasion by smaller, soluble prions. Acta Neuropathol. Commun. 5, 32.

Binyamin, O., et al., 2015. Treatment of a multiple sclerosis animal model by a novel nanodrop formulation of a natural antioxidant. Int. J. Nanomedicine 10, 7165–7174.

Braidy, N., et al., 2016. Consumption of pomegranates improves synaptic function in a transgenic mice model of Alzheimer's disease. Oncotarget 7, 64589–64604.

Canello, T., et al., 2010. Oxidation of helix-3 methionines precedes the formation of PK resistant PrP. PLoS Pathog. 6, e1000977.

Caughey, B., Baron, G.S., 2006. Prions and their partners in crime. Nature 443, 803–810.

Czub, M., et al., 1988. Replication of the scrapie agent in hamsters infected intracerebrally confirms the pathogenesis of an amyloid-inducing virosis. J. Gen. Virol. 69 (Pt 7), 1753–1756.

Dhopeshwarkar, G.A., Mead, J.F., 1973. Uptake and transport of fatty acids into the brain and the role of the blood-brain barrier system. Adv. Lipid Res. 11, 109–142.

Diaz-Nido, J., et al., 2002. Glycosaminoglycans and beta-amyloid, prion and tau peptides in neurodegenerative diseases. Peptides 23, 1323–1332.

Fainstein, N., et al., 2016. Chronic progressive neurodegeneration in a transgenic mouse model of prion disease. Front. Neurosci. 10, 510.

Friedman-Levi, Y., et al., 2011. Fatal prion disease in a mouse model of genetic E200K Creutzfeldt-Jakob disease. PLoS Pathog. 7, e1002350.

Friedman-Levi, L., et al., 2013. PrPST, a soluble, protease resistant and truncated PrP form features in the pathogenesis of a genetic prion disease. PLoS One 8 (7), e69583. http://dx.doi.org/10.1371/journal.pone.0069583.

Gabizon, R., et al., 1987. Purified prion proteins and scrapie infectivity copartition into liposomes. Proc. Natl. Acad. Sci. U. S. A. 84, 4017–4021.

Geschwind, M.D., et al., 2013. Quinacrine treatment trial for sporadic Creutzfeldt-Jakob disease. Neurology 81, 2015–2023.

Halliday, M., et al., 2017. Repurposed drugs targeting eIF2alpha-P-mediated translational repression prevent neurodegeneration in mice. Brain.

Hijazi, N., et al., 2005. PrPSc incorporation to cells requires endogenous glycosaminoglycan expression. J. Biol. Chem. 280 (17), 17057–17061.

Hinz, F.I., Geschwind, D.H., 2017. Molecular genetics of neurodegenerative dementias. Cold Spring Harb. Perspect. Biol. 9 (4). http://dx.doi.org/10.1101/cshperspect.a023705.

Imamura, M., et al., 2016. Heparan sulfate and heparin promote faithful prion replication in vitro by binding to normal and abnormal prion proteins in protein misfolding cyclic amplification. J. Biol. Chem. 291, 26478–26486.

Imberdis, T., et al., 2016. Identification of anti-prion compounds using a novel cellular assay. J. Biol. Chem. 291, 26164–26176.

Jurenka, J.S., 2008. Therapeutic applications of pomegranate (*Punica granatum* L.): a review. Altern. Med. Rev. 13, 128–144.

Kaplan, M., Aviram, M., 2001. Retention of oxidized LDL by extracellular matrix proteoglycans leads to its uptake by macrophages: an alternative approach to study lipoproteins cellular uptake. Arterioscler. Thromb. Vasc. Biol. 21, 386–393.
Karapetyan, Y.E., et al., 2013. Unique drug screening approach for prion diseases identifies tacrolimus and astemizole as antiprion agents. Proc. Natl. Acad. Sci. U. S. A. 110, 7044–7049.
Kocisko, D.A., Caughey, B., 2006a. Mefloquine, an antimalaria drug with antiprion activity in vitro, lacks activity in vivo. J. Virol. 80, 1044–1046.
Kocisko, D.A., Caughey, B., 2006b. Searching for anti-prion compounds: cell-based high-throughput in vitro assays and animal testing strategies. Methods Enzymol. 412, 223–234.
Kovacs, G.G., et al., 2010. Genetic Creutzfeldt-Jakob disease associated with the E200K mutation: characterization of a complex proteinopathy. Acta Neuropathol. 121, 39–57.
Lasmezas, C.I., et al., 1997. Transmission of the BSE agent to mice in the absence of detectable abnormal prion protein. Science 275, 402–405.
Lesne, S.E., et al., 2013. Brain amyloid-beta oligomers in ageing and Alzheimer's disease. Brain 136, 1383–1398.
Liu, S., et al., 2015. The neuroprotective effects of resveratrol preconditioning in transient global cerebral ischemia-reperfusion in mice. Turk. Neurosurg. 26, 550–555.
Loren, D.J., et al., 2005. Maternal dietary supplementation with pomegranate juice is neuroprotective in an animal model of neonatal hypoxic-ischemic brain injury. Pediatr. Res. 57, 858–864.
May, B.C., et al., 2003. Potent inhibition of scrapie prion replication in cultured cells by bisacridines. Proc. Natl. Acad. Sci. U. S. A. 100, 3416–3421.
Mayer-Sonnenfeld, T., et al., 2005. The metabolism of glycosaminoglycans is impaired in prion diseases. Neurobiol. Dis. 20, 738–743.
Mayer-Sonnenfeld, T., et al., 2008. Chemically induced accumulation of GAGs delays PrP(Sc) clearance but prolongs prion disease incubation time. Cell. Mol. Neurobiol. 28, 1005–1015.
Mizrahi, M., et al., 2014. Pomegranate seed oil nanoemulsions for the prevention and treatment of neurodegenerative diseases: the case of genetic CJD. Nanomedicine 10, 1353–1363.
Mota Ferreira, L., et al., 2016. Pomegranate seed oil nanoemulsions with selective antiglioma activity: optimization and evaluation of cytotoxicity, genotoxicity and oxidative effects on mononuclear cells. Pharm. Biol. 54, 2968–2977.
Palinski, W., et al., 1996. Cloning of monoclonal autoantibodies to epitopes of oxidized lipoproteins from apolipoprotein E-deficient mice. Demonstration of epitopes of oxidized low density lipoprotein in human plasma. J. Clin. Invest. 98, 800–814.
Papy-Garcia, D., et al., 2011. Glycosaminoglycans, protein aggregation and neurodegeneration. Curr. Protein Pept. Sci. 12, 258–268.
Peretz, D., et al., 2001. Antibodies inhibit prion propagation and clear cell cultures of prion infectivity. Nature 412, 739–743.
Prusiner, S.B., 2013. Biology and genetics of prions causing neurodegeneration. Annu. Rev. Genet. 47, 601–623.
Raymond, G.J., et al., 2006. Inhibition of protease-resistant prion protein formation in a transformed deer cell line infected with chronic wasting disease. J. Virol. 80, 596–604.
Sawant, R.R., Torchilin, V.P., 2010. Multifunctionality of lipid-core micelles for drug delivery and tumour targeting. Mol. Membr. Biol. 27, 232–246.
Schonberger, O., et al., 2003. Novel heparan mimetics potently inhibit the scrapie prion protein and its endocytosis. Biochem. Biophys. Res. Commun. 312, 473–479.
Shaked, G.M., et al., 2001. Reconstitution of prion infectivity from solubilized protease-resistant PrP and nonprotein components of prion rods. J. Biol. Chem. 276, 14324–14328.
Sharma, D.R., et al., 2016. Quercetin attenuates neuronal death against aluminum-induced neurodegeneration in the rat hippocampus. Neuroscience 324, 163–176.
Silber, B.M., et al., 2014. Novel compounds lowering the cellular isoform of the human prion protein in cultured human cells. Bioorg. Med. Chem. 22, 1960–1972.
Silveira, J.R., et al., 2005. The most infectious prion protein particles. Nature 437, 257–261.
Snow, A.D., et al., 1989. Sulfated glycosaminoglycans in amyloid plaques of prion diseases. Acta Neuropathol. 77, 337–342.
Spector, R., 1988. Fatty acid transport through the blood-brain barrier. J. Neurochem. 50, 639–643.
Subash, S., et al., 2014. Pomegranate from Oman alleviates the brain oxidative damage in transgenic mouse model of Alzheimer's disease. J. Tradit. Complement. Med. 4, 232–238.
Suzuki, K., et al., 1997. Mice deficient in all forms of lysosomal beta-hexosaminidase show mucopolysaccharidosis-like pathology. J. Neuropathol. Exp. Neurol. 56, 693–703.
Tomatsu, S., et al., 2013. Newborn screening and diagnosis of mucopolysaccharidoses. Mol. Genet. Metab. 110, 42–53.
Velusamy, T., et al., 2017. Protective effect of antioxidants on neuronal dysfunction and plasticity in Huntington's disease. Oxidative Med. Cell. Longev. 2017, 3279061.
Vieira, T.C., et al., 2014. Heparin binding confers prion stability and impairs its aggregation. FASEB J. 28, 2667–2676.
Wang, F., et al., 2017. Self-propagating, protease-resistant, recombinant prion protein conformers with or without in vivo pathogenicity. PLoS Pathog. 13, e1006491.
Wong, C., et al., 2001. Sulfated glycans and elevated temperature stimulate PrP(Sc)-dependent cell-free formation of protease-resistant prion protein. EMBO J. 20, 377–386.
Ye, X., 2009. Visual pathology in animal prion diseases. Histol. Histopathol. 24, 1563–1577.
Yin, S., et al., 2007. Human prion proteins with pathogenic mutations share common conformational changes resulting in enhanced binding to glycosaminoglycans. Proc. Natl. Acad. Sci. U. S. A. 104, 7546–7551.
Zhou, M., et al., 2015. Neuronal death induced by misfolded prion protein is due to NAD+ depletion and can be relieved in vitro and in vivo by NAD+ replenishment. Brain 138, 992–1008.